Prospective Cohort Study

INTERNATIONAL JOURNAL OF SURGERY

OPEN

Prognostic implication of residual inflammatory trajectories in acute type I aortic dissection: dual-center prospective cohort study

Hong Liu, MD, PhD[a,*], Yi-fei Diao, MD[a], Yong feng Shao, MD, PhD[a,*], Si-chong Qian, MD, PhD[b,*], Zhi-hua Zeng, MD, PhD[c], Guo-liang Fan, MD[d], Lu-yao Ma, MD, PhD[a], Hong-jia Zhang, MD, PhD[b]; on the behalf of the Additive Anti-inflammatory Action for Aortopathy & Arteriopathy (5A) Investigators

Background: Peripheral platelet-white blood cell ratio (PWR) integrating systemic inflammatory and coagulopathic pathways is a key residual inflammatory measurement in the management of acute DeBakey type I aortic dissection (AAD); however, trajectories of PWR in AAD is poorly defined.

Methods: Two AAD cohorts were included in two cardiovascular centers (2020–2022) if patients underwent emergency total arch replacement with frozen elephant trunk implantation. PWR data were collected over time at baseline and five consecutive days after surgery. Trajectory patterns of PWR were determined using the latent class mixed modelling (LCMM). Cox regression was used to determine independent risk factors. By adding PWR Trajectory, a user-friendly nomogram was developed for predicting mortality after surgery.

Results: Two hundred forty-six patients with AAD were included with a median follow-up of 26 (IRQ 20–37) months. Three trajectories of PWR were identified [cluster α 45(18.3%), β105 (42.7%), and γ 96 (39.0%)]. Cluster γ was associated with higher risk of mortality at follow-up (crude HR, 3.763; 95% CI: 1.126–12.574; $P = 0.031$) than cluster α. By the addition of PWR trajectories, an inflammatory nomogram, composed of age, hemoglobin, estimated glomerular filtration rate, and cardiopulmonary time was developed and internally validated, with adequate discrimination [the area under the receiver-operating characteristic curve 0.765, 95% CI: 0.660–0.869)], calibration, and clinical utility.

Conclusion: Based on PWR trajectories, three distinct clusters were identified with short-term outcomes, and longitudinal residual inflammatory shed some light to individualize treatment strategies for AAD.

Keywords: inflammatory, latent class extend mixed model, trajectory, type I aortic dissection

Introduction

DeBakey type I aortic dissection is a lethal cardiovascular emergency with a high incidence and early mortality[1,2]. Currently, total arch replacement combined frozen elephant trunk (FET) implantation is a well-established treatment option for this type of aortic dissection[3]. Because of the heterogeneity of this cardiovascular catastrophe, risk stratification and early treatment initiation is important for clinical decision-making and prognosis evaluation. Recently, the International Registry of Acute Aortic Dissection (IRAD) score[4] and German Registry for Acute Aortic Dissection Type A (GERAADA) score[5] have been developed as predictive models of surgical risk of aortic dissection, which are useful for predicting 30-day or in-hospital mortality but not long-term prognosis.

It is well suggested that inflammation plays pivotal role in the initiation, progression, and surgical repair of AAD. A variety of inflammatory biomarkers have increasingly attracted attention as

[a]Department of Cardiovascular Surgery, The First Affiliated Hospital of Nanjing Medical University, Nanjing, [b]Department of Cardiovascular Surgery, Beijing Anzhen Hospital, Capital Medical University, Beijing, [c]Department of Cardiovascular Surgery, The Second Affiliated Hospital of Nanchang University, Nanchang and [d]Department of Critical Care Medicine, Shanghai East Hospital, Tongji University School of Medicine, Shanghai, People's Republic of China

Sponsorships or competing interests that may be relevant to content are disclosed at the end of this article.

*Corresponding author. Address: Department of Cardiovascular Surgery, The First Affiliated Hospital of Nanjing Medical University, Nanjing 210029, People's Republic of China. Tel.: +86 188 012 81613. E-mail: dr.hongliu@foxmail.com (H. Liu), and Tel.: +86 025 683 03101. E-mail: yfshaojph@sina.com (Y.-F. Shao); Department of Cardiovascular Surgery, Beijing Anzhen Hospital, Capital Medical University, Beijing 100029, People's Republic of China. Tel.: +86 131 201 30755. E-mail: drqsc1990a@163.com (S.-C. Qian).

International Journal of Surgery (2024) 110:3346–3356

Received 21 December 2023; Accepted 21 February 2024

Supplemental Digital Content is available for this article. Direct URL citations are provided in the HTML and PDF versions of this article on the journal's website, www.lww.com/international-journal-of-surgery.

Published online 4 March 2024

http://dx.doi.org/10.1097/JS9.0000000000001245

predictive and prognostic indicators in AAD patients[6,7]. Bedel and Selvi[8] reported that a high platelet-lymphocyte ratio at admission was associated with increased in-hospital mortality in patients with AAD. However, Xie *et al.*[9] suggested that U-shaped relationship between platelet-lymphocyte ratio and in-hospital mortality in AAD patients. Previously, our observations demonstrated that an integrated index of coagulation/inflammatory pathways (platelet-white blood cell ratio, PWR) before surgery was associated with adverse outcomes following aortic dissection surgery[10–14]. Perioperative dynamic monitoring of peripheral PWR could provide a more comprehensive and accurate assessment of systemic inflammatory and thrombotic reactions, which can help physicians better understand the disease status and characteristics of this specific diseases. However, the effect of perioperative trajectory of this index among AAD patients is unexplored.

The purpose of this study was to determine PWR trajectories over time in patients with AAD who underwent surgical repair in the real-world setting, and further to explore the potential implication of residual inflammatory trajectories in risk stratifications for individualized decision-making.

HIGHLIGHTS

- Three distinct trajectories of peripheral platelet-white blood cell ratio were identified (cluster α, β, and γ).
- Cluster γ (a decline trajectory) was associated with higher risk of mortality than cluster α (a table trajectory).
- The addition of platelet-white blood cell ratio trajectories into base nomogram (age, hemoglobin, estimated glomerular filtration rate, and cardiopulmonary time) improved the discrimination.

Methods

Patients

Between January 2020 and May 2022, patients hospitalized to the Department of Cardiovascular Surgery at the two cardiovascular centers were prospectively included. All patients fulfilled the DeBakey classification criteria for aortic dissection and had aortic computed tomography angiography confirmed AAD. Those patients were included if they underwent emergency total arch repair and FET implantation at hospital admission and survive more than 5 days after this current surgery. Those patients were excluded if they were chronic dissection or aneurysm of aorta, traumatic or iatrogenic aortic dissection, had regional or systemic infection in the last month before surgery, and received with only endovascular or medical management. All patients provided written informed consent. The work has been reported in line with the strengthening the reporting of cohort, cross-sectional, and case–control studies in Surgery (STROCSS) criteria[15] (Supplemental Digital Content 1, http://links.lww.com/JS9/C55).

Data collection

At baseline, the following data was collected: demographic information, medical history, and laboratory tests, as well as procedural profiles. PWR measurements (defined as the count of platelet to white blood cell ratio) from baseline to the last laboratory test up to 4 days after this surgery were subjected to trajectory analysis. In detail, data were collected at six consecutive time points on each case (T0: hospital admission, T1: ICU admission immediately after surgery, T2: first morning after surgery, T3: second morning after surgery, T4: third morning after surgery, and T5: forth morning after surgery). Importantly, estimated glomerular filtration rate (eGFR) was calculated with 2021 CKD-EPI Creatinine Equation (https://www.kidney.org/professionals/kdoqi/gfr_calculator/formula). To avoid insufficient elapsed time to generate a PWR trajectory and to reduce the potential for survival bias, those patients who died with the first 4 days after surgery were excluded from this analysis. Laboratories in the two hospitals were certificated via the National Accreditation Service for Conformity Assessment, which ensures consistency and homogeneity of laboratory results. Those patients missing five serial measurements postoperatively were excluded.

Procedure

Cardiopulmonary bypass (CPB) was instituted by cannulating either on the right axillary or on the innominate arteries, in which the latter was preferred if the innominate artery was free of dissection or serious atherosclerosis. The ascending aorta was clamped and transected at the cooling phase, and Del Nido cardioplegia was directly infused into the orifice of left and right coronary arteries. When the cooling temperature reached the target temperature of 21–23°C in the bladder, circulatory arrest of lower body was launched by unilateral antegrade cerebral perfusion at a flow rate of 5.0 ml/kg/min. Frozen elephant trunk graft was antegradely inserted into the true lumen of the descending aorta. Then, the stented graft and the descending aorta was anastomosed end-to-end with 4-branched graft. Once the distal anastomosis was finished, perfusion in the lower body was resumed through the 4-branched graft. Subsequently, the second branch of 4-branched graft was anastomosed with the left common carotid artery to restore the left cerebral perfusion as quickly, followed by rewarming. The left subclavian artery was anastomosed with the third branch of 4-branched graft via the same fashion. Then, the proximal ascending aorta was anastomosed with the proximal end of the 4-branched graft. After deairing, the cross-clamp was removed and the innominate artery was anastomosed with the first branch. At last, CPB was weaned off under stable hemodynamic parameters, and this was followed by complete protamine neutralization[16].

Outcomes

The primary outcome was all-cause mortality at follow-up, defined as any death, regardless of cause, occurring during follow-up up to 31 October 2023 after surgery in or out of the hospital. The follow-up was completed on the last medical interview date, the last examination date, or the date when the endpoint event was observed, whichever came first. All-cause mortality at 30 days was also investigated to assess an association of clusters with a short-term endpoint, defined as any death, regardless of cause, occurring within 30 days after surgery in or out of the hospital, and after 30 days during the same hospitalization subsequent to the operation according to the Society of Thoracic Surgeons criteria[17]. Other outcomes included the mechanical ventilation duration,

ICU length of stay, and hospital length of stay. All alive patients were followed up until 31 October 2023.

Statistical analysis

Latent class mixture model (LCMMs) is a mathematical algorithm used to classify individuals on the basis of longitudinal repeated measures to uncover subpopulations with distinct trends over time. In this present study, mixed effects models with random intercepts were fitted in the 'lcmm' R package with PWR as the dependent variable[18]. The optimal number of classes was determined by Bayesian information criterion (BIC)[19]. Model adequacy was measured with the average of posterior probability of assignments and odds of correct cluster.

We summarized the baseline, clinical and procedural characteristics and perioperative outcomes of the entire cohort and between latent classes. Statistics are presented as means with SD or medians with interquartile range [IQR] for continuous variables, and frequencies and proportions for categorical variables. Continuous data was compared by Kruskal–Wallis test. Categorical data was compared by Pearson's χ^2 test with Yates' continuity correction or Fisher's exact test if appropriate.

A Cox proportional hazards model was used to investigate the associations between exposures (distinct PWR trajectories) and the risks of mortality at last follow-up with hazards ratio (HR) with a 95% CI. The Kaplan–Meier survival curve and the log-rank test were used to estimate and compare survival times. Univariable and multivariable Cox regression models were fitted to identify statistically independent predictors of mortality at last follow-up. First, a univariable Cox regression analysis was used to quantify the association of each potential determinant with mortality at follow-up and for inclusion in multivariable regression analysis. Then, variables with a *P*-value <0.10 in the univariable analysis were included in the multivariable regression analysis. At last, these significant variables with a *P*-value of <0.05 was considered as independent predictors in the multivariable analysis. Based on the results of multivariable analysis, a nomogram to predict mortality at 3 months, 12 months, 24 months, and 36 months of follow-up was developed by integration of candidate variables ($P < 0.05$). Model performance was assessed by examining discrimination [the area under the receiver-operating characteristic curve (AUROC)], calibration (Hosmer–Lemeshow test and visually by plotting the predicted probability against the actual observed frequency of mortality), and the clinical utility (decision curve analysis)[20–22]. A nomogram was developed for graphical presentation of the models. Internal validation of the model was evaluated using Efron's enhanced bootstrap method. This method is chosen above other methods of model validation because it allows for the development of the most stable prediction model in a limited number of research participants[23]. In brief, the model was internally validated using 1000 bootstrap samples. Bias-corrected 95% CI were obtained from bootstrap samples. The optimism-corrected AUROC, which provides a measure of the extent to which the original model is too optimistic, or overfits the data, was calculated by generating the difference between the original AUROC and the AUROC obtained from each bootstrap sample, taking this difference from the original AUROC and averaging this across the bootstrap samples[24,25]. Additional analyses were performed to explore whether ulinastatin use modified the association between distinct PWR trajectories and the risks of mortality. All statistical analyses were performed using STATA software version 13.0. *P*-values <0.05 were considered statistically significant.

Results

Patients' characteristics

A total of 246 patients were included finally (Supplemental Figure 1, Supplemental Digital Content 2, http://links.lww.com/JS9/C56), with 178 (72.4%) males, the median (IQR) age of 55 (45–63) year, the median (IQR) time from onset to emergency surgery of 10[5–18] hours and 68 (27.6%) patients received ulinastatin. Of 246 patients, three (1.2%) cases underwent aortic valve replacement, 36 (14.6%) cases underwent Bentall procedure, and 11 (4.5%) cases underwent David procedure. The median (IQR) time of cardiopulmonary bypass, aortic clamp, and hypothermic circulatory arrest was 194 (173–231) mins, 147 (121–179) mins, and 18 (15–24) mins, respectively. Baseline, clinical, and procedural characteristics are listed in Table 1. The median follow-up time was 26 (IQR 20–37) months among AAD patients alive. Sequential PWR over time was showed in Supplemental Figure 2 (Supplemental Digital Content 2, http://links.lww.com/JS9/C56).

Three-cluster trajectory model

LCMM analysis revealed that three-cluster trajectory model provided the best fit, which effectively represented distinct longitudinal patterns of PWR in AAD patients (Fig. 1). Three-cluster trajectory had the lowest BIC value and demonstrated adequate clinical sensibility, as indicated in Supplemental Table 1–2 (Supplemental Digital Content 2, http://links.lww.com/JS9/C56) and Supplemental Figures 3–4 (Supplemental Digital Content 2, http://links.lww.com/JS9/C56).

According to LCMM analysis, a total of 45 patients (18.3%) were assigned to Cluster α, characterized by a stable trajectory of PWR with lower levels at the beginning and remaining relatively stable over time. Cluster β consisted of 105 patients (42.7%) with a U-shaped trajectory, where PWR gradually decreased and then rose again over time. Cluster γ included 96 patients (39.0%) with a decreasing trajectory, where PWR gradually decreased over time (Fig. 1 and Supplemental Figure 3A, B, Supplemental Digital Content 2, http://links.lww.com/JS9/C56). Patients in Cluster γ exhibited the lowest percentage of males [57 (59.4%)], the highest PWR at baseline [median 15.7 (11.1–21.0)], the lowest hemoglobin level [134.0 (118.0–147.2) g/l], the highest platelet count [183.5 (141.0–225.5) × 10^9/l], and the highest WBC count [11.3 (8.5–14.5) × 10^9/l] compared to those in Clusters α and β. No significant differences were observed in terms of clinical risk factors and biochemical profiles among the three clusters (Table 1).

Outcomes in three latent clusters

Cluster γ was associated with higher risk of mortality at follow-up (crude HR, 3.763; 95% CI: 1.126–12.574; $P = 0.031$) than cluster α. However, there was no significant difference in mortality between cluster α and cluster β. After pooling cluster α and cluster β, cluster γ was also associated with higher risk of mortality at follow-up (crude HR, 2.879; 95% CI: 1.450–5.715; $P = 0.003$) compared with cluster α and cluster β. Kaplan–Meier survival curves illustrate differences in mortality among the three trajectory clusters in Figure 2.

Table 1

Patient characteristics and outcomes of the entire cohort and each trajectory group.

	Overall (*N* = 246)	α (*N*1 = 45)	β (*N*2 = 105)	γ (*N*3 = 96)	*P*
Baseline characteristics					
Age (years)	55.0 (45.0–62.8)	54.0 (47.0–62.0)	54.0 (45.0–60.0)	55.5 (45.8–64.0)	0.511
Sex male, *n* (%)	178 (72.4%)	40 (88.9%)	81 (77.1%)	57 (59.4%)	< 0.001
Height (cm)	170.0 (165.0–175.0)	171.0 (167.0–175.0)	170.0 (165.0–175.0)	170.0 (161.8–175.0)	0.837
Weight (kg)	75.0 (64.0–80.0)	75.0 (70.0–81.0)	75.0 (65.0–80.0)	71.0 (60.0–80.0)	0.196
Bosy surface area (m^2)	2.0 (1.8–2.0)	2.0 (1.9–2.1)	2.0 (1.8–2.1)	1.9 (1.8–2.0)	0.243
BMI (kg/m^2)	25.4 (23.3–27.7)	25.6 (23.9–27.7)	25.8 (23.4–27.8)	24.8 (22.9–27.5)	0.246
Clinical characteristics					
Smoking, *n* (%)	42 (17.1%)	7 (15.6%)	16 (15.2%)	19 (19.8%)	0.662
Alcohol drinking, *n* (%)	37 (15.0%)	3 (6.7%)	13 (12.4%)	21 (21.9%)	0.038
Hypertension, *n* (%)	190 (77.2%)	36 (80.0%)	80 (76.2%)	74 (77.1%)	0.877
Diabetes mellitus, *n* (%)	5 (2.0%)	0 (0.0%)	1 (1.0%)	4 (4.2%)	0.154
Chronic lung disease, *n* (%)	28 (11.4%)	5 (11.1%)	10 (9.5%)	13 (13.5%)	0.668
Coronary heart disease, *n* (%)	6 (2.4%)	1 (2.2%)	1 (1.0%)	4 (4.2%)	0.335
Stroke, *n* (%)	12 (4.9%)	1 (2.2%)	6 (5.7%)	5 (5.2%)	0.649
Leukocyte count over time					
Leukocyte ($\times 10^9$/l) T0	12.4 (9.7–15.2)	13.4 (10.9–17.1)	12.5 (10.5–15.0)	11.3 (8.5–14.5)	0.020
Leukocyte ($\times 10^9$/l) T1	11.2 (9.3–13.6)	10.2 (9.3–12.2)	11.3 (9.1–13.6)	11.6 (9.7–14.8)	0.044
Leukocyte ($\times 10^9$/l) T2	11.6 (9.8–14.6)	9.9 (7.7–11.2)	12.0 (9.9–14.7)	12.2 (10.3–16.1)	< 0.001
Leukocyte ($\times 10^9$/l) T3	11.9 (9.7–14.7)	10.0 (8.3–13.9)	11.6 (10.1–14.0)	12.7 (10.5–16.1)	0.002
Leukocyte ($\times 10^9$/l) T4	10.7 (8.8–13.7)	9.9 (8.1–11.8)	9.9 (8.5–11.8)	12.3 (10.3–15.7)	< 0.001
Leukocyte ($\times 10^9$/l) T5	10.1 (8.3–12.7)	9.4 (8.3–11.2)	8.9 (7.6–10.8)	12.3 (9.9–15.2)	< 0.001
Platelet count over time					
Platelet ($\times$109/l) T0	168.0 (132.0–206.8)	141.0 (116.0–182.0)	165.0 (133.0–205.0)	183.5 (141.0–225.5)	0.022
Platelet ($\times$109/l) T1	103.0 (79.2–127.8)	99.0 (77.0–124.0)	105.0 (82.0–130.0)	104.5 (79.8–123.0)	0.695
Platelet ($\times$109/l) T2	88.5 (63.2–114.8)	88.0 (68.0–115.0)	92.0 (69.0–116.0)	86.5 (54.5–113.2)	0.025
Platelet ($\times$109/l) T3	74.5 (53.2–102.8)	84.0 (61.0–127.0)	82.0 (57.0–103.0)	65.0 (48.0–82.0)	< 0.001
Platelet ($\times$109/l) T4	75.0 (54.0–109.0)	85.0 (70.0–128.0)	93.0 (67.0–121.0)	60.5 (42.8–78.2)	< 0.001
Platelet ($\times$109/l) T5	93.5 (63.0–132.8)	99.0 (78.0–145.0)	117.0 (91.0–150.0)	68.0 (43.0–92.0)	< 0.001
Platelet-leukocyte ratio over time					
Platelet-leukocyte ratio T0	14.0 (10.3–17.5)	10.4 (8.2–14.8)	13.7 (10.6–16.1)	15.7 (11.1–21.0)	< 0.001
Platelet-leukocyte ratio T1	9.0 (7.2–11.5)	9.9 (7.9–12.9)	9.1 (7.5–11.9)	8.6 (6.9–10.7)	0.330
Platelet-leukocyte ratio T2	7.7 (5.3–10.0)	9.9 (6.6–13.8)	7.5 (5.4–9.6)	7.0 (3.9–9.4)	< 0.001
Platelet-leukocyte ratio T3	6.5 (4.1–9.2)	8.5 (6.7–13.8)	7.2 (5.1–9.2)	4.7 (3.3–7.3)	< 0.001
Platelet-leukocyte ratio T4	7.5 (4.5–10.7)	10.1 (6.8–13.6)	9.1 (6.4–11.4)	4.9 (3.2–7.1)	< 0.001
Platelet-leukocyte ratio T5	9.9 (5.4–14.3)	11.2 (7.4–16.1)	12.6 (10.3–17.1)	5.3 (3.4–7.8)	< 0.001
Laboratory profiles					
Hemoglobin (g/l)	136.5 (124.0–148.0)	144.0 (132.0–150.0)	137.0 (126.0–148.0)	134.0 (118.0–147.2)	0.046
Blood urea nitrogen (mmol/l)	6.8 (5.4–8.4)	6.8 (5.3–8.8)	7.0 (5.9–8.2)	6.5 (5.2–8.3)	0.464
Creatinine (μmol/l)	77.7 (60.5–98.4)	76.5 (62.1–99.2)	79.0 (60.1–96.5)	75.0 (60.6–102.5)	0.497
eGFR ($ml/min/1.73m^2$)	96.3 (71.0–120.5)	101.5 (84.5–114.1)	97.1 (72.5–128.6)	94.8 (65.0–120.3)	0.261
Aspartate aminotransferase (u/l)	28.4 (23.0–37.8)	30.3 (25.3–37.0)	27.6 (22.1–38.1)	28.6 (22.8–37.2)	0.503
Alanine aminotransferase (u/l)	29.4 (22.6–42.2)	29.4 (23.2–38.5)	31.0 (24.1–42.5)	28.7 (21.2–42.2)	0.555
Albumin (g/l)	39.0 (37.7–40.5)	38.5 (37.8–40.5)	39.0 (37.3–40.5)	39.1 (37.9–40.5)	0.813
De Ritis ratio	1.0 (0.8–1.2)	1.0 (0.8–1.2)	0.9 (0.7–1.2)	1.0 (0.8–1.3)	0.089
Lactate (mmol/l)	1.6 (0.9–3.5)	1.5 (0.8–2.4)	1.5 (1.0–3.5)	1.6 (0.9–3.6)	0.434
Procedural characteristics					
Root procedure (%)					0.147
Aortic valve replacement, *n* (%)	3 (1.2%)	0 (0.0%)	1 (1.0%)	2 (2.1%)	
Bentall, *n* (%)	36 (14.6%)	6 (13.3%)	13 (12.4%)	17 (17.7%)	
David, *n* (%)	11 (4.5%)	1 (2.2%)	3 (2.9%)	7 (7.3%)	
CPB time (min)	194 (173–231)	183 (161–220)	186 (171–210)	217 (180–265)	0.002
Aortic clamp time (min)	147 (121–179)	135 (105–158)	142 (120–164)	154 (139–190)	0.024
Circulatory arrest time (min)	18 (15–24)	20 (16–24)	18 (13–24)	18 (15–23)	0.765
CABG, *n* (%)	7 (2.8%)	1 (2.2%)	1 (1.0%)	5 (5.2%)	0.186
Concomitant surgery[a], *n* (%)	6 (2.4%)	1 (2.2%)	1 (1.0%)	4 (4.2%)	0.335
Anti-inflammatory pharmacotherapy					
Ulinastatin use	68 (27.6%)	14 (31.1%)	32 (30.5%)	22 (22.9%)	0.414
Outcomes					
Follow-up time (months)	26 (20–37)	28 (22–37)	30 (21–38)	25 (4–36)	0.023
Mortality at last follow-up, *n* (%)	35 (14.2%)	3 (6.7%)	10 (9.5%)	22 (22.9%)	0.007
Mortality at 30 days, *n* (%)	24 (9.8%)	2 (4.4%)	8 (7.6%)	14 (14.6%)	0.104

Table 1

(Continued)

	Overall ($N=246$)	α ($N1=45$)	β ($N2=105$)	γ ($N3=96$)	*P*
Circulatory failure	6 (2.44%)	1 (2.22%)	2 (1.90%)	3 (3.13%)	
Neurologic dysfunction	2 (0.81%)	0	1 (0.95%)	1 (1.04%)	
Ventricular arrhythmia	3 (1.22%)	0	1 (0.95%)	2 (2.08%)	
Infection	3 (1.22%)	0	1 (0.95%)	2 (2.08%)	
Respiratory failure	4 (1.63%)	1 (2.22%)	1 (0.95%)	2 (2.08%)	
Renal failure	2 (0.81%)	0	1 (0.95%)	1 (1.04%)	
Hepatic failure	1 (0.41%)	0	0	1 (1.04%)	
Gastrointestinal hemorrhage	3 (1.22%)	0	1 (0.95%)	2 (2.08%)	
Mechanical ventilation time (hours)	65 (28–143.5)	63 (22–153)	58 (28–131)	70 (33–150)	0.242
ICU stay (days)	9 (6–16)	9.0 (5–13)	9 (5–14)	10 (7–19)	0.036
Hospital stays (days)	21 (16–31)	22 (17–32)	20 (15–26)	22 (17–36)	0.015

Data are mean (SD), *n* (%) or median (IQR).
CABG, coronary artery bypass grafting; CPB, Cardiopulmonary bypass; eGFR, estimated glomerular filtration rate.
[a]Concomitant one of the following procedures: mitral or tricuspid valve surgery.

The results remain similar after adjusting for baseline, clinical and procedural variables known to be associated with mortality (Table 2). No significant differences was observed in term of all-cause mortality at 30 days between three latent clusters (Supplemental Table 3, Supplemental Digital Content 2, http://links.lww.com/JS9/C56 and Fig. 2). Other perioperative outcomes were showed in Table 1.

Predictors of mortality at follow-up

In the univariable analysis, age, BMI, eGFR, hgb, Albumin, De Ritis ratio, and CPB time were found to have *P*-value <0.10 and were considered for inclusion in the final model, except aortic clamp time, which was removed due to multicollinearity (Table 3). Finnlay, age, eGFR, hemoglobin, and cardiopulmonary bypass (CPB) time in the multivariable model were found to be a significant predictor of mortality ($P<0.05$).

Incremental prognostic value of adding PWR trajectory

Based on the conventional independent risk factors (age, eGFR, hgb, and CPB time), we developed a nomogram (base model) to predict the probability of mortality at 3 months, 12 months, 24 months, and 36 months of follow-up (Fig. 3A). By addition of PWR trajectory to this base model, we further developed an inflammatory nomogram for risk prediction (Fig. 3B).

ROC curve showed the inflammatory nomogram has better discrimination accuracy than base nomogram [AUROC=0.765,

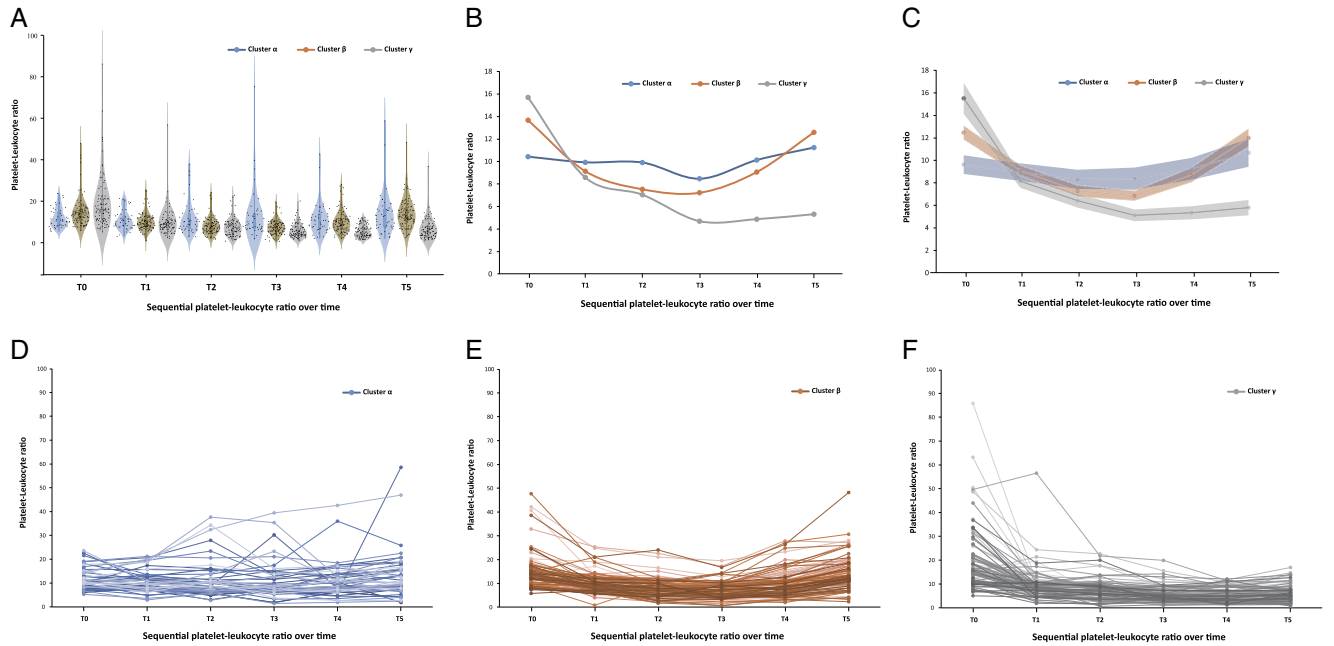

Figure 1. Three trajectories of PWR in Type I Aortic Dissection. (A) Violin plot showing summary statistics of PWR for three cluster over time; (B) Trajectory plots with median of PWR for three cluster over time; (C) Trajectory plots with average and 95% predictive intervals of PWR for each cluster; (D) Spaghetti plots of PWR of each patient over time in cluster α; (E) Spaghetti plots of PWR of each patient over time in cluster β; (F) Spaghetti plots of PWR of each patient over time in cluster γ. PWR, platelet-white blood cell ratio.

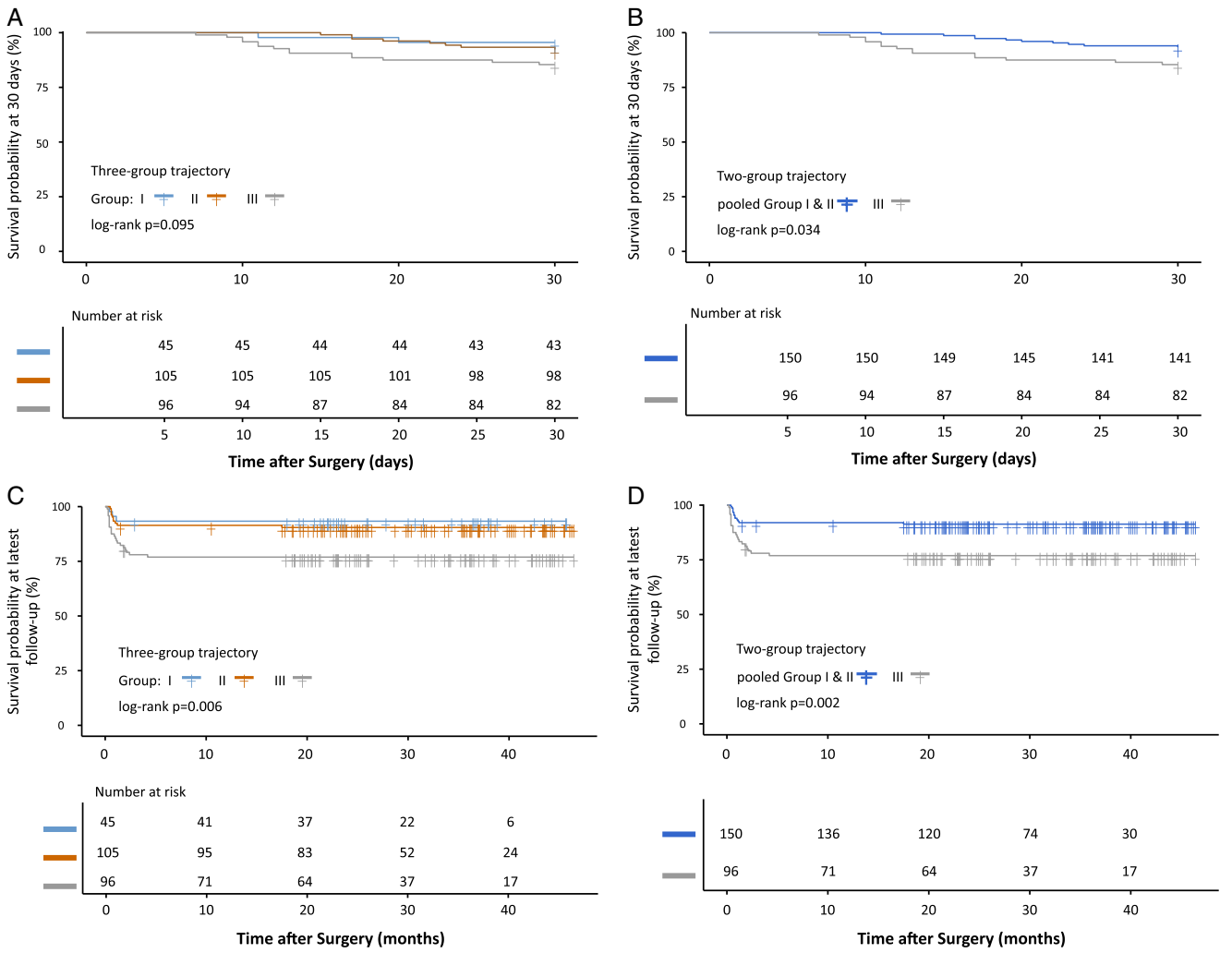

Figure 2. Kaplan–Meier curve among PWR trajectory. A: Kaplan–Meier curve at 30 days among cluster α, β, and γ; B: Kaplan–Meier curve at 30 days among pooled cluster α and β and cluster γ; C: Kaplan–Meier curve at latest follow-up among cluster α, β, and γ; D: Kaplan–Meier curve at latest follow-up among pooled cluster α and β and cluster γ. PWR, platelet-white blood cell ratio.

95% CI: 0.660–0.869 vs. 0.726 (0.616–0.837), Fig. 3C, D]. The Hosmer–Lemeshow test for two model calibration gave a *P*-value of 0. 326 and 0.438, respectively, and calibration curves also indicated that there was no significant difference between the observed and predicted probabilities of mortality (Fig. 3E, F). The decision curve analysis indicates that the inflammatory model has better clinical benefit and making treatment decisions using inflammatory model has a higher net benefit than base nomogram for mortality between the risk threshold of 15–60% (Fig. 3G, H). For the two nomograms, the specificity and sensitivity of base nomogram was 0.579 and 0.808, and of inflammatory nomogram was 0.790 and 0.731, respectively.

Internal validation of the model

To assess the model's performance further, the enhanced Bootstrap method was used for internal validation. The model development dataset was resampled 1000 times with replacement, resulting in 1000 datasets of equal sample size. The bias-corrected AUROC through internal validation by bootstrapping 1000 samples was 0.716 for base mode and 0.756 for inflammatory models, which are approximately similar with the original models before bootstrapping, respectively, (Fig. 4). Besides, the optimism coefficients of base and inflammatory models were found to be 0.004 and 0.004, respectively, indicating robust discriminative performance even after internal validation.

Additional analysis

Overall, a trend existed for decreased mortality at last follow-up when ulinastatin was used [HR 0.539 (95% CI: 0.224–1.297), *P* = 0.167] without reaching significant differences (Supplemental Table 4, Supplemental Digital Content 2, http://links.lww.com/JS9/C56). By analysis of trajectory cluster and treatment effect, a trend also existed for decreased mortality at last follow-up when ulinastatin was used in each cluster despite no statistical differences. Alluvial plot showed distribution of three trajectory clusters across ulinastatin use and mortality at the last follow-up (Supplemental Figure 5, Supplemental Digital Content 2, http://links.lww.com/JS9/C56). The results remain similar after

Table 2

Results of Cox proportional hazard model assessing the effect of platelet-leukocyte ratio trajectory group on mortality at last follow-up.

	Hazard ratio (95% CI)	P
Mortality at last follow-up		
Unadjusted		
α ($N_1 = 45$)	1.0 (ref.)	
β ($N_2 = 105$)	1.440 (0.396–5.232)	0.580
γ ($N_3 = 96$)	3.763 (1.126–12.574)	0.031
Adjusted for baseline and clinical factors		
α ($N_1 = 45$)	1.0 (ref.)	
β ($N_2 = 105$)	1.418 (0.385, 5.222) 6	0.599
γ ($N_3 = 96$)	3.726 (1.097, 12.656)	0.035
Adjusted for baseline, clinical, and procedural factors		
α ($N_1 = 45$)	1.0 (ref.)	
β ($N_2 = 105$)	1.480 (0.398, 5.502)	0.558
γ ($N_3 = 96$)	3.954 (1.153, 13.557)	0.028
Mortality at last follow-up		
Unadjusted		
Pooled α and β ($N_{1+2} = 150$)	1.0 (ref.)	
γ ($N_3 = 96$)	2.879 (1.450–5.715)	0.003
Adjusted for baseline and clinical factors		
Pooled α and β ($N_{1+2} = 150$)	1.0 (ref.)	
γ ($N_3 = 96$)	2.875 (1.443–5.728)	0.003
Adjusted for baseline, clinical, and procedural factors		
Pooled α and β ($N_{1+2} = 150$)	1.0 (ref.)	
γ ($N_3 = 96$)	2.965 (1.464–6.006)	0.003

adjusting for baseline, clinical and procedural variables known to be associated with mortality (Supplemental Table 4, Supplemental Digital Content 2, http://links.lww.com/JS9/C56).

Discussion

In this real-world setting of AAD patients, three distinct trajectories of residual inflammatory trajectories were identified using a semi-supervised machine learning approach. This is the first study, to the best of our knowledge, to delineate the longitudinal patterns of systemic inflammation and coagulation function following total arch replacement and FET implantation. Cluster γ was independently associated with a significantly increased risk of mortality at last follow-up than cluster α. By the addition of three trajectories of PWR, an inflammatory nomogram was developed for mortality prediction, with adequate discrimination, calibration, and clinical applicability.

Identification of three trajectories of PWR is of clinical significance, since the distinct trajectories of PWR were closely associated with short-term and mid-term mortality. Of note, distinguishing cluster γ from other clusters (clusters α and β) is of great clinical interest. Compared with clusters α only or pooled cluster α and β, cluster γ represented the highest risk of mortality at 30 days and at last follow-up. For those patients of cluster γ, either the gradual increase of WBC count or the gradual decline of the platelet counts in peripheral blood over time contributes to worsening the inflammatory process as well as progressive deterioration of coagulation function. From the perspective of clinical feasibility and practicality, the nature of PWR determines its advantageous aspects in providing timely and useful information for both diagnostic and therapeutic decision-making, due to its easy availability in both emergency setting and daily clinical practice.

Although baseline PWR is a well-conceived important factor, the predictive value alone is only moderate accuracy in predicting mortality after surgery of AAD[6,10]. Based on our hypothesis that AAD is heterogeneous cardiovascular syndrome[26], we use semi-supervised machine learning approach (latent class mixture model) to characterize the longitudinal patterns of PWR over time by baseline and five consecutively postoperative PWR values. As expected, we identified three distinct and clinically relevant clusters by analyzing PWR trajectories, and a decline trajectory was associated with higher short-term and mid-term mortality compared with stable trajectory. Also, the result remains similar after adjustment of baseline, clinical and procedural confounders. When we deal with AAD that is dynamic, changing with physiological, pathological, and environmental conditions and interventional procedures, dynamic grouping principle contributes increasing efficiency and flexibility in solving highly complex problems[27].

Consistent with previous reports, age, hemoglobin, eGFR, and CPB time proved to be significant independent prognostic factors in multivariable analysis[6,10–14,28,29]. Compared with baseline platelet and WBC count, our findings showed PWR has superior discrimination ability to individual hematologic parameter in predicting mortality following AAD surgery. By the addition of PWR trajectory to conventional risk factors, an inflammatory nomogram was derived and internally validated for prediction of mortality. Importantly, our model was developed for risk evaluations at the result of the mid-term follow-up, which was different from the existing risk models that focus on short-term mortality, such as 30-day mortality and in-hospital mortality, with its simplicity of requiring only five items as a major advantage. All predictors included in nomogram for risk stratification are routinely measured during hospitalization, making the score available at any facility. Besides, all patients included were surgically repaired by senior surgeons at high-volume cardiovascular centers in which total arch replacement and FET implantation was standardized, which minimizes variability in the interpretation of results[30].

Limitation

Our study has some limitations. First, our analysis was limited by the small numbers of patients, it likely leads to the lack of enough power for determination of differences between clusters. Second, given the developed nomogram is not externally validated, more evidence and external validation in different populations is wanted to address the generalizability issue in the future. Third, in consideration of the nature of the emergency setting and retrospective study, some features of importance, for example, cytokines and immunological profiles, are not included in this present study, which is likely to contribute to enhancing the prediction performance of this inflammatory nomogram. So, more novel biomarkers should be explored and integrated into the conventional risk models to empower the discrimination.

Table 3

Univariate and multivariate cox regression analyses to determine the independent predictors of mortality at the last time of follow-up.

	Univariate		Multivariate	
	Hazard ratio (95% CI)	*P*	Hazard ratio (95% CI)	*P*
Age (years)	1.027 (0.998–1.056)	0.064	1.030 (1.001–1.060)	0.041
Sex				
Female	1.0 (reference)			
Male	0.697 (0.347–1.400)	0.310		
BMI (Kg/m^2)	0.918 (0.837–1.007)	0.068	0.924 (0.842–1.014)	0.095
Smoking				
No	1.0 (reference)			
Yes	1.477 (0.671–3.251)	0.332		
Alcohol drinking				
No	1.0 (reference)			
Yes	1.759 (0.799–3.872)	0.160		
Hypertension				
No	1.0 (reference)			
Yes	0.730 (0.351–1.520)	0.400		
Diabetes mellitus				
No	1.0 (reference)			
Yes	1.454 (0.584–3.616)	0.421		
Stroke				
No	1.0 (reference)			
Yes	2.049 (0.627–6.693)	0.234		
Chronic lung disease				
No	1.0 (reference)			
Yes	1.650 (0.685–3.974)	0.264		
Coronary heart disease				
No	1.0 (reference)			
Yes	2.484 (0.596–10.355)	0.211		
White blood cell (×109/l)	1.031 (0.953–1.116)	0.446		
Hemoglobin (g/l)	0.985 (0.968–1.002)	0.083	0.991 (0.983–1.000)	0.039
Platelet (×109/l)	0.995 (0.989–1.002)	0.150		
Creatinine (μmol/l)	1.000 (0.997–1.002)	0.897		
Blood urea nitrogen (mmol/l)	1.000 (0.942–1.061)	0.995		
eGFR (ml/min/1.73m^2)	0.984 (0.975–0.993)	0.0006	0.986 (0.976–0.995)	0.004
Alanine aminotransferase (u/l)	1.001 (0.999–1.003)	0.236		
De Ritis ratio	1.630 (0.951–2.792)	0.075	1.603 (0.922–2.787)	0.094
Albumin (g/l)	0.842 (0.732–0.969)	0.016	0.881 (0.758–1.023)	0.096
PWR trajectory cluster				
α	1.0 (reference)		1.0 (reference)	
β	1.440 (0.396–5.232)	0.579	1.410 (0.388–5.132)	0.601
γ	3.763 (1.126–12.574)	0.031	3.547 (1.049–11.996)	0.041
CPB time (min)	1.007 (1.003–1.011)	0.002	1.008 (1.003–1.013)	0.0008
Aortic clamp time (min)	1.007 (1.001–1.013)	0.026	1.010 (1.002–1.018)	0.019
Circulatory arrest time (min)	1.024 (0.972–1.078)	0.374		
Root procedures				
None	1.0 (reference)			
Aortic valve replacement	3.360 (0.447–25.267)	0.239		
Root replacement	1.199 (0.497–2.893)	0.685		
CABG				
No	1.0 (reference)			
Yes	2.224 (0.533–9.274)	0.272		
Concomitant surgery[a]				
No	1.0 (reference)			
Yes	2.587 (0.621–10.784)	0.191		

CABG, coronary artery bypass grafting; CPB, Cardiopulmonary bypass; eGFR, estimated glomerular filtration rate.
[a]Concomitant one of the following procedures: mitral or tricuspid valve surgery.

Conclusions

In patients with AAD, three distinct clusters integrating systemic inflammatory and coagulopathic pathways were identified using a semi-supervised machine learning approach. Declining PWR cluster was associated with higher risk of mortality. By the addition of PWR cluster into conventional risk factors, we provide a superior-performance, user-friendly risk model to predict short-term mortality

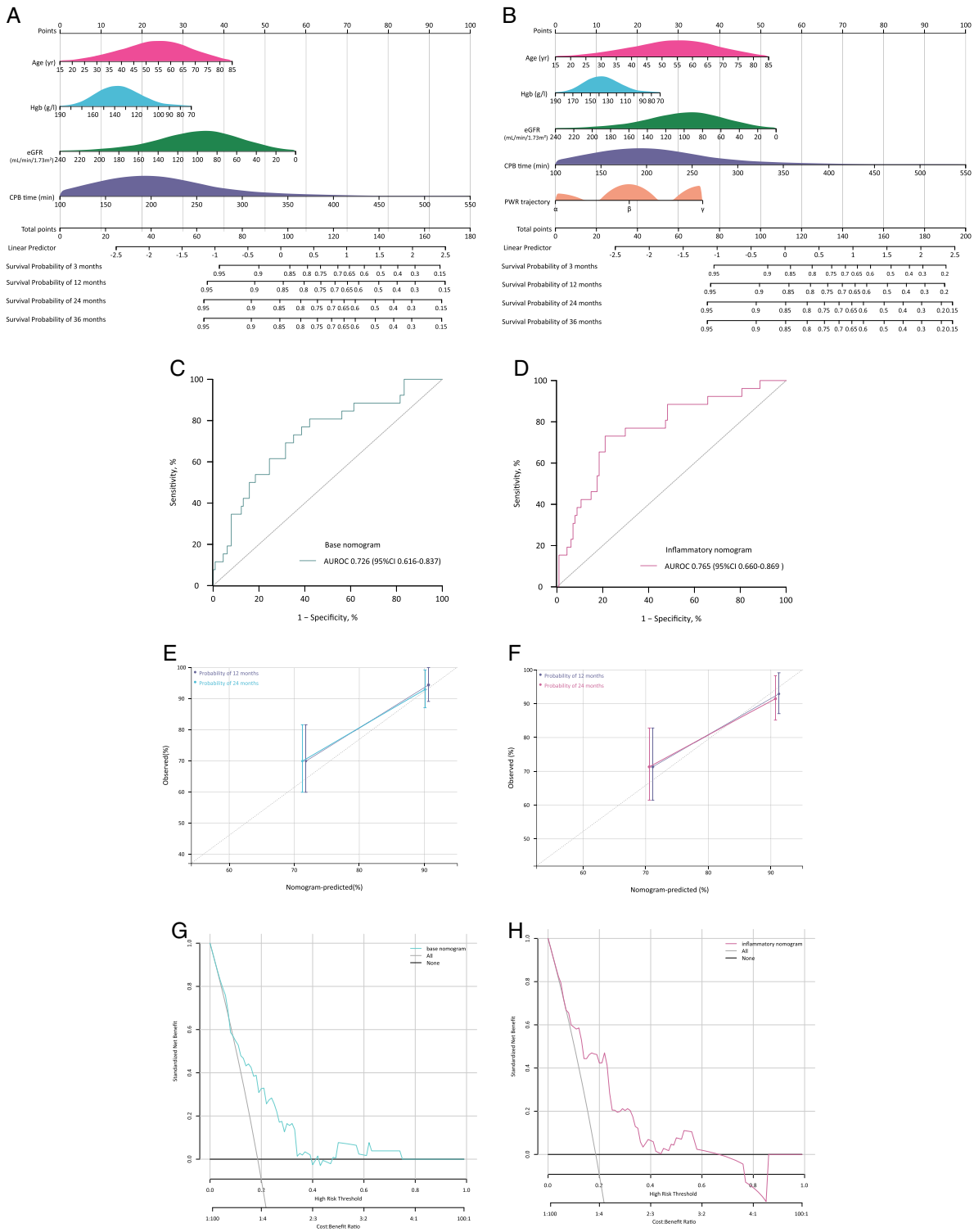

Figure 3. Derivation and assessment of nomograms for mortality prediction. A, B: Base and inflammatory nomogram for mortality predictions; C, D: AUROCs of base and inflammatory nomogram; E, F: Calibration plots of base and inflammatory nomogram; G, H: Clinical decision curves of base and inflammatory nomogram. AUROC, the area under the receiver-operating characteristic curves.

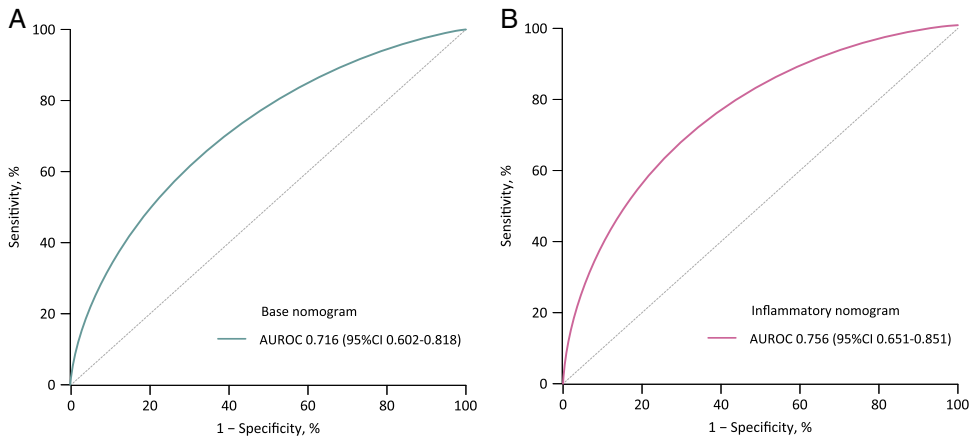

Figure 4. Internal verification of nomograms after bootstrapping. A: AUROC of base nomogram; B: AUROC of inflammatory nomogram. AUROC. the area under the receiver-operating characteristic curves.

following total arch replacement and FET implantation. Longitudinal trajectories integrating systemic inflammatory and coagulopathic pathways shed some light to optimize treatment strategies for AAD via tailored anti-inflammatory pharmacotherapeutics.

Ethical approval

This study was approved by the Institutional Review Board of the First Affiliated Hospital of Nanjing Medical University (no. 2021-SR-381) and the Institutional Review Board of the Beijing Anzhen Hospital of Capital Medical University (KS2022034). All patients provided informed consent.

Consent

All patients provided written informed consent.

Sources of funding

This work was supported in part by the Scientific Research Common Program of Beijing Municipal Commission of Education (KM202110025014), Jiangsu Province Capability Improvement Project through Science, Technology and Education (ZDXK202230), and Public Welfare Project of Nanjing Medical University Alliance for Specific Diseases (JZ23349020230306).

Author contribution

H.L.: had the idea of the study, conceptualized the research aims; H.L., S.C.Q., Y.F.S., and H.J.Z.: design the study and take responsibility for the integrity of the data and the accuracy of the data analysis. All authors contributed to the acquisition of data. H.L. and S.C.Q.: doing the statistical analysis; H.L. and S.C.Q.: wrote the first draft of the paper, and other authors provided comments and approved the final manuscript. H.L., S.C.Q., G.L.F., and Y.F.S.: revised the paper.

Conflicts of interest disclosure

None.

Research registration unique identifying number (UIN)

1. Name of the registry: https://www.clinicaltrials.gov/
2. Unique identifying number or registration ID: NCT04398992.
3. Hyperlink to your specific registration (must be publicly accessible and will be checked): https://clinicaltrials.gov/ct2/show/NCT04398992.

Guarantor

Hong Liu.

Data availability statement

Data are available on reasonable request. The data are confidential and not publicly available. The codes and notebooks are available on reasonable request to the authors.

Provenance and peer review

Not commissioned, externally peer-reviewed.

Investigator-initiated Additive Anti-inflammatory Action for Aortopathy & Arteriopathy (5A) Investigators

Hong Liu MD, PhD, Department of Cardiovascular Surgery, the First Affiliated Hospital of Nanjing Medical University, Nanjing 210029, P.R China.

Acknowledgements

Assistance with the study: none.
Presentation: none.

References

[1] Bossone E, Eagle KA. Epidemiology and management of aortic disease: aortic aneurysms and acute aortic syndromes. Nat Rev Cardiol 2021;18:331–48.

[2] Malaisrie SC, Szeto WY, Halas M, *et al*. 2021 The American Association for Thoracic Surgery expert consensus document: Surgical treatment of acute type A aortic dissection. J Thorac Cardiovasc Surg 2021;162:735–58.

[3] Sun L, Qi R, Zhu J, *et al*. Total arch replacement combined with stented elephant trunk implantation: a new "standard" therapy for type a dissection involving repair of the aortic arch? Circulation 2011;123:971–8.

[4] Rampoldi V, Trimarchi S, Eagle KA, *et al*. Simple risk models to predict surgical mortality in acute type A aortic dissection: the international registry of acute aortic dissection score. Ann Thorac Surg 2007;83:55–61.

[5] Czerny M, Siepe M, Beyersdorf F, *et al*. Prediction of mortality rate in acute type A dissection: the German registry for acute type A aortic dissection score. Eur J Cardiothorac Surg 2020;58:700–6.

[6] Liu H, Li H, Han L, *et al*. Inflammatory risk stratification individualizes anti-inflammatory pharmacotherapy for acute type A aortic dissection. Innovation (Camb) 2023;4:100448.

[7] Tsilimigras DI, Sigala F, Karaolanis G, *et al*. Cytokines as biomarkers of inflammatory response after open versus endovascular repair of abdominal aortic aneurysms: a systematic review. Acta Pharmacol Sin 2018;39:1164–75.

[8] Bedel C, Selvi F. Association of platelet to lymphocyte and neutrophil to lymphocyte ratios with In-Hospital mortality in patients with type A acute aortic dissection. Braz J Cardiov Surg 2019;34:694–8.

[9] Xie X, Fu X, Zhang Y, *et al*. U-shaped relationship between platelet-lymphocyte ratio and postoperative in-hospital mortality in patients with type A acute aortic dissection. BMC Cardiovasc Disord 2021;21:569.

[10] Liu H, Qian SC, Han L, *et al*. Circulating biomarker-based risk stratifications individualize arch repair strategy of acute Type A aortic dissection via the XGBoosting algorithm. Eur Heart J Digit Health 2022;3:587–99.

[11] Liu H, Qian SC, Shao YF, *et al*. Prognostic impact of systemic coagulation-inflammation index in acute type A aortic dissection surgery. JACC Asia 2022;2:763–76.

[12] Liu H, Qian SC, Zhang YY, *et al*. A novel inflammation-based risk score predicts mortality in acute type A aortic dissection surgery: the additive anti-inflammatory action for aortopathy and arteriopathy score. Mayo Clin Proc Innov Qual Outcomes 2022;6:497–510.

[13] Zhao HL, Tang ZW, Diao YF, *et al*. Inflammatory profiles define phenotypes with clinical relevance in acute type A aortic dissection. J Cardiovasc Transl Res 2023;16:1383–91.

[14] Liu H, Qian SC, Shao YF, *et al*. Anti-inflammatory effect of ulinastatin on the association between inflammatory phenotypes in acute type A aortic dissection. J Inflamm Res 2022;15:3709–18.

[15] Mathew G, Agha R. for the STROCSS Group. STROCSS 2021: strengthening the reporting of cohort, cross-sectional and case-control studies in surgery. Int J Surg 2021;96:106165.

[16] Dong Z, Liu H, Kim JB, *et al*. False lumen-dependent segmental arteries are associated with spinal cord injury in frozen elephant trunk procedure for acute type I aortic dissection. JTCVS Open 2023;15:16–24.

[17] Carrel T, Sundt TM III, von Kodolitsch Y, *et al*. Acute aortic dissection. Lancet 2023;401:773–88.

[18] Proust-Lima C, Philipps V, Liquet B. Estimation of extended mixed models using latent classes and latent processes: the R Package lcmm. J Stat Softw 2017;78:1–56.

[19] Nagin DS. Group-Based Modeling of Development. Cambridge: Harvard University Press; 2005.

[20] Meurer WJ, Tolles J. Logistic regression diagnostics: understanding how well a model predicts outcomes. JAMA 2017;317:1068–9.

[21] Alba AC, Agoritsas T, Walsh M, *et al*. Discrimination and calibration of clinical prediction models: users. Guides to the medical literature. JAMA 2017;318:1377–84.

[22] Vickers AJ, Elkin EB. Decision curve analysis: a novel method for evaluating prediction models. Med Decis Making 2006;26:565–74.

[23] Fernandez-Felix BM, García-Esquinas E, Muriel A, *et al*. Bootstrap internal validation command for predictive logistic regression models. Stata J 2021;21:498–509.

[24] Hu R, Wu B, Wang C, *et al*. Assessment of transient elastography in diagnosing MAFLD and the early effects of sleeve gastrectomy on MAFLD among the chinese population. Int J Surg 2024. doi:10.1097/JS9.0000000000001078. [Online ahead of print].

[25] Jackson AM, Goland S, Farhan HA, *et al*. A novel score to predict left ventricular recovery in peripartum cardiomyopathy derived from the ESC EORP Peripartum Cardiomyopathy Registry. Eur Heart J 2024. Published online January 29. doi:10.1093/eurheartj/ehad888. [Online ahead of print].

[26] Lansman SL, Saunders PC, Malekan R, *et al*. Acute aortic syndrome. J Thorac Cardiovasc Surg 2010;140(6 Suppl):S92–7.

[27] Vilacosta I, San Román JA, di Bartolomeo R, *et al*. Acute AORTIC SYNDROME REVISITED: JACC state-of-the-art review. J Am Coll Cardiol 2021;78:2106–25.

[28] Xing L, Zhou Y, Han Y, *et al*. Simple death risk models to predict in-hospital outcomes in acute aortic dissection in emergency department. Front Med (Lausanne) 2022;9:890567.

[29] An Z, Zhong K, Sun Y, *et al*. Risk factors for in-hospital mortality after total arch procedure in patients with acute type A aortic dissection. Front Cardiovasc Med 2023;10:1149907.

[30] Liu H, Zhang YY, Ding XH, *et al*. Proximal vs extensive repair in acute type A aortic dissection surgery. Ann Thorac Surg 2023;116:270–8.